

Syngas-fueled, chemical-looping combustion-based power plant lay-out for clean energy generation

R. J. Basavaraj · S. Jayanti

Received: 27 February 2014 / Accepted: 5 May 2014 / Published online: 24 May 2014
© Springer-Verlag Berlin Heidelberg 2014

Abstract Of the various clean combustion technologies with carbon capture and sequestration (CCS) possibilities, chemical-looping combustion (CLC) promises to be an efficient and attractive method for oxidizing fuels without the energy penalty required for oxygen separation from air. The present work reports on a detailed thermodynamic analysis of 1,500 MWth, syngas-fueled, CLC-based power generation system which includes a provision for CCS. Taking account of the exothermic nature of the reaction of syngas with the selected oxygen carrier, NiO, in the fuel reactor, operating temperatures of air and fuel reactors are fixed at 900 and 908 °C, respectively. The CLC reactor system operates at atmospheric pressure on fuel/air side, and generates supercritical steam. An overall plant lay-out has been prepared such that the steam side, which is rated at 240 bar/538/552/566 °C, is very similar to that of a conventional thermal power plant making retrofitting a distinct possibility. A detailed analysis of the ideal cycle shows that a highly promising gross cycle efficiency of 41.22 % and net cycle efficiency of 36.77 % can be achieved after accounting for the energy cost of CO₂ compression to 110 bar to facilitate CCS.

Keywords Chemical-looping combustion · Syngas · Oxygen carrier · CO₂ capture · Supercritical steam · Retrofit

Notation

CLC Chemical-looping combustion
T Temperature at any point, °C

CLCSC Chemical-looping combustion steam cycle
T_r Reference temperature, °C
M_i Mass flow of component i, kg/s
C_{Pm} Heat capacity of metal, kJ/kg.K
m Mass flow of gas or liquid in Table 2, kg/s
a, b, c & d Coefficients of temperature polynomial in Eq. (9)
C_{Pi} Heat capacity of component i, kJ/kg.K
h Enthalpy, kJ/kg
q_{Air in} Thermal energy flow in air entering the air reactor, kW
q_{Depleted air} Thermal energy flow in oxygen-depleted air, kW
q_{MeOx} Thermal energy flow in oxygenated metal oxide, kW
q_{Me} Thermal energy flow in reduced form of metal oxide, kW
q_{Ox} Thermal energy produced by metal oxidation reaction, kW
q_{ARExtract} Thermal energy extracted from air reactor by cooling fluid, kW
q_{Fuel in} Thermal energy flow in fuel entering the air reactor, kW
q_{Red} Heat produced by metal reduction reaction, kW
m_{fuel} Mass flow rate of fuel, kg/s
LHV_{fuel} Lower heating value of fuel, MJ/kg
P_{steam turbine} Total power produced by CLCSC steam turbines, MW
P_{water pump} Power consumed to pump water at required pressure, MW
P_{CO₂comp} Power consumed for carbon dioxide compression, MW
η_{Gross} Gross efficiency of CLCSC power plant
η_{Net} Net efficiency of CLCSC power plant

R. J. Basavaraj · S. Jayanti (✉)
Department of Chemical Engineering, IIT Madras,
Chennai 600036, India
e-mail: sjayanti@iitm.ac.in

HE1 Steam super heat exchanger
 HE2, HE3 Steam reheaters

Subscript

MeO Metal oxide
 Me Reduced form of metal oxide
 e Electrical (related to power, as in MW_e)
 AR Air reactor
 Ox Oxidation
 Red Reduction
 r Reference
 m, n Oxidized and reduced states of O₂ carrier, respectively
 th Thermal (related to power, as in MW_{th})

Greek symbols

α, β & γ Coefficients of temperature polynomial in Eq. (10)

Introduction

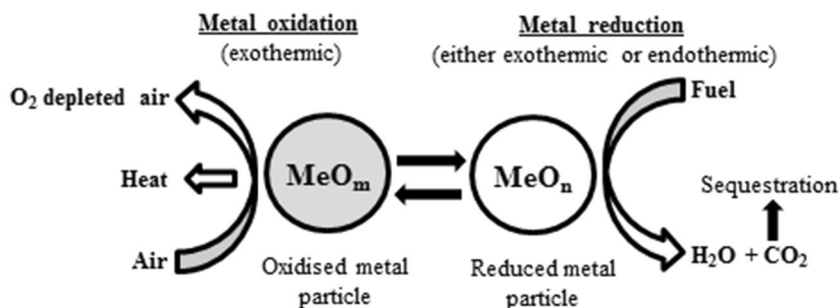
The emission of carbon dioxide from thermal power plants is a matter of considerable concern for policy makers and energy providers all over the world. At present, combustion of fossil fuels based sectors accounts for around 80 % of primary energy production (IEA 2006) and account for more than a third of the anthropogenic CO₂ emissions (IPCC 2005). There are several advantages with fossil fuels from a power generation point of view, and while efforts are going on to make power generation greener (see the recent summary of Yan et al. 2013), it is expected that countries such as India will continue to depend significantly on coal-based power generation for the next few decades (Chikkatur et al. 2007; Jayanti et al. 2012; Krishna Priya and Bandyopadhyay 2013). Apart from thermal power stations, energy-intensive industries such as steel plants and cement plants also release significant amounts of CO₂ into the atmosphere (IPCC 2005). In view of these continued emissions of CO₂ from normal human activities and the harmful consequence in terms of global warming, there has been tremendous interest in recent years on means of carbon capture and sequestration (CCS) with special focus on capture of combustion-related CO₂ emissions. A number of ways of pre- and post-combustion capture techniques have been proposed; recent reviews have been provided by Wall (2007), Davison and Thambimuthu (2009) and Kanniche et al. (2010), among others. While post-combustion capture of CO₂ from flue gases has received wide attention due to the maturity of the technology in other fields and continues to do so (see for example, Bandyopadhyay 2011; Damartzis et al. 2014), oxy-fuel combustion and its variants (Wall et al. 2009;

Seepana and Jayanti 2009; Sivaji and Jayanti 2010) are being considered as a less-energy-intensive way of carbon capture (Liszka and Ziebig 2010; Jayanti et al. 2012). Several non-technical aspects, primarily economical and political, related to CCS have also been receiving increasing attention of late. Jenni et al. (2013) recently reported on an estimate of the energy penalties associated with various carbon capture technologies and concluded these methods levied a significant efficiency penalty on the thermal power generation process. Hasaneen et al. (2014) reported on the microeconomic and political impact of imposing carbon tax to finance CCS. In view of the cost increases associated with CCS, Loughlin et al. (2013) considered the possibility of future breakthrough technologies for mitigating CO₂ and proposed a methodology for assessing new developments from this perspective.

In recent years, chemical-looping combustion (CLC), originally proposed for green house gas capture by Ishida et al. (1987) and Ishida and Jin (1994), has been attracting attention as a more cost-effective, though technologically as yet immature, way of carbon capture. As shown by Ishida et al. (1987) through energy analysis, CLC results in significantly reduced energy loss compared to conventional or oxy-fuel combustion, which raises the prospect of lesser thermal efficiency penalty for carbon capture. The principle of chemical-looping combustion is illustrated in Fig. 1. Here, the combustion of a hydrocarbon fuel is carried out in two stages. Firstly, a metal (or a metal oxide in which the metal is in a low oxidation state) is brought into contact with air at high temperature so that a metal oxide or a higher oxide is formed by selective reaction with oxygen contained in air. In the second stage, the metal oxide reacts with the hydrocarbon fuel and gives up its oxygen (partly or fully) to oxidize the carbon in the fuel to carbon dioxide and the hydrogen to water vapor. These reactions are carried out typically at high temperatures in separate air and fuel reactors, respectively. The hot product gases from the reactors are taken through separate streams for heat recovery and sequestration/disposal as applicable.

The two-stage combustion of the hydrocarbon fuel eliminates the need for oxygen separation from air which is required in oxy-fuel combustion, and it also prevents the contamination of the product gas of the fuel reactor with nitrogen. The exhaust from the fuel reactor will primarily be CO₂ and water vapor; the latter can be easily separated through condensation leaving a nearly pure stream of CO₂, which can, therefore, be sent directly for compression for eventual storage. The first chemical-looping-based power generation system was proposed in 1994 by Ishida and Jin (1994) and details of the two-step gas–solid combustion were studied by Hatanaka et al. (1997). A major effort was made by the Grangemouth Advanced CO₂ Capture Project in which initial laboratory-scale experimentation with

Fig. 1 Chemical-looping combustion principle



newly found oxygen carriers was reported by Lyngfelt et al. (2004); kinetics and reactivity of the oxygen carriers were reported by Adánez et al. (2004) and Adánez et al. (2005) and issues related to scaling up to pilot plant level were reported by Kronberger et al. (2004). At present, a number of CLC demonstration units are being operated in laboratories worldwide. A 1-MW_{th} CLC-based power plant is being operated at Institute of Energy System and Technology at Technische Universität Darmstadt (Ströhle et al. 2013). A 100 kW_{th} capacity chemical-looping combustor is under operation in Chalmers University of Technology (Markström et al. 2013). A compact 25 kW_{th} moving bed CLC reactor is under demonstration at Ohio State University (Tong et al. 2013). National Energy Technology Laboratory is constructing a pressurized 250 kW_{th} pilot plant unit funded by the United States Department of Energy (Tong et al. 2013). Experiments in lab-scale CLC units of thermal ratings of 0.3 kW_{th} (Moldenhauer et al. 2013), 1.5 kW_{th} (Adánez-Rubio et al. 2013), and 10 kW_{th} (Mayer et al. 2013) are also under operation.

The basic parameters of CLC systems, in terms of the useful oxygen carriers and their operating temperatures for various gaseous fuels, are now well understood and a number of studies are being conducted to investigate optimal reactor configurations. A comprehensive review of the current status of chemical-looping combustion is given by Adánez et al. (2012). The objective of the present work is to study the system lay-out for practical power generation applications with special emphasis on syngas. The choice of syngas is appropriate for two reasons. A number of emerging nations such as India, China, and South Africa have huge future energy requirements, but do not have vast reserves of natural gas, while their proven coal reserves can last for the next 100–200 years. Secondly, syngas or gas containing a mixture of combustible gases such as CO, CH₄, and H₂ of sufficient calorific value may be produced from a number of biomass and alternative fuel sources which are actively being sought across the globe. These sources may often be seasonal and linking a gasifier to a thermal power plant may be difficult. What is envisaged, therefore, is a delinking of the two; it is assumed in the study that syngas of known composition and calorific value

is available and the objective to use it in a CLC-based thermal power generation systems so as to enable implementation of CCS. The focus is, therefore, on the lay-out of a syngas-fired CLC plant. The purpose of this study is to identify the primary and secondary energy recovery sources to generate high pressure and high temperature steam required for efficient and sustainable power generation. Details of the system lay-out and its thermodynamic analysis are discussed below.

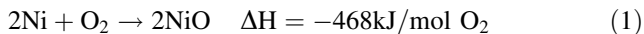
Choice of the CLC parameters

Choice of the oxygen carrier

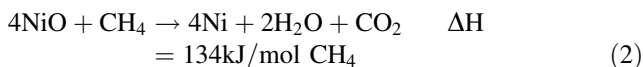
Oxygen carriers are the key component in CLC technology. An oxygen carrier that is to be used in a continuously operated in CLC environment has to meet a number of requirements, the most important of which are suitable properties for use in a fluidized-bed reactor, physical and chemical stability at high temperature operation in oxidizing and reducing environments, high conversion of hydrocarbon fuels, and sufficient rates of oxidation and reduction. Several metal/metal oxide pairs have been investigated for potential use as oxygen carriers in CLC. Among these, nickel oxides have proved to be one of the most promising oxygen carriers for CLC due to their high reactivity, good oxygen transport capacity, and great chemical stability. Nickel-based oxygen carriers are capable of converting CH₄, H₂, or CO upto 99.5 % (Linderholm et al. 2008). Ni-based oxygen carriers can be used at high temperatures of 900–1,100 °C in a CLC process which enables a sufficiently high temperature operation of the steam cycle. Generally speaking, the reactivity of the four most studied supported oxygen carriers is in the descending order: NiO > CuO > Mn₂O₃ > Fe₂O₃ (Johansson 2007). In view of these observations, NiO/NiAl₂O₄ with a nickel content of 60 % by weight is considered as the oxygen carrier in the present study.

The two-stage combustion of the hydrocarbon fuel is carried out in two separate reactors. In the air reactor (AR), Ni is made to react with air to form NiO. This is then made

to react with a hydrocarbon fuel in the fuel reactor (FR) to complete the oxidation of the fuel. The oxidation of nickel in the AR is highly exothermic:



when the hydrocarbon fuel is syngas, NiO reacts with the fuel components CH₄, CO, and H₂ as per the reactions (2), (3), and (4), respectively (Adánez et al. 2012):



The heats of reaction have been estimated at the reactor operating temperatures (typically in the range of 900–1000 °C) from data cited in the literature (Linderholm et al. 2008; Adánez et al. 2012). Here, one may note that CH₄ oxidation reaction is endothermic, while CO and H₂ oxidation reactions by NiO are mildly exothermic. Since the proportion of CO and H₂ is relatively high in syngas compared to that of CH₄, the overall syngas oxidation reaction in FR is mildly exothermic.

Reactor configuration

Unlike in the case of normal air combustion, the oxidation of syngas in CLC is a two-step heterogeneous reaction, each involving a gas–solid phase reaction. In order to prevent high velocities (leading to possible loss of catalyst through attrition and to avoid erosion of heat exchanger tubes), the two reactions are carried out in two fluidized-bed reactors. The overall configuration of the CLC “furnace” is shown schematically in Fig. 2. It is composed of two reactors: an AR or metal oxidation reactor and a FR or metal oxide reduction reactor. Air is introduced into the circulating fluidized bed (CFB) AR containing oxygen carrier metal Ni, and reacts to form NiO during pneumatic transport of metal particles as per reaction (1) with release of heat. The metal oxide (NiO) particles are separated from the oxygen-depleted air in a cyclone. They pass through loop seals to enter the FR where they are reduced by different components of syngas as per reactions (2)–(4). Metal oxide reduction reaction is slow and requires high residence time to react with fuel. Therefore, the FR is operated in bubbling fluidized-bed mode. The reduced Ni particles are then sent to the air reactor for oxidation. The overall oxygen carrier flow diagram is highlighted schematically in Fig. 2. The dots indicate metal or metal oxide particles. The dark dot indicates fully oxygenated state, the lightly-shaded dot indicates partially oxidized state, and an empty circle indicates reduced state of the oxygen carrier particles. During these cyclic redox reactions in the fuel and the ARs,

hot exit gases consisting of CO₂ rich exhaust gases and oxygen-depleted air are released from the air and the FRs, respectively. These are used to preheat the gases entering the respective reactors. Heat available from the tail gases can also be used for preheating the water. A large portion of the heat produced in the AR is extracted for steam generation using the in-bed/embedded heat exchangers. The supercritical boiler in the AR will be similar to the once-through type of supercritical boilers being currently used in large CFB power plants (IEA 2013; VTT 2013). The exit gases from the reactors and the preheating heat exchangers serve as “economizers” of a corresponding steam boiler, while the in-bed/embedded heat exchangers are used for superheating and reheating the steam.

Thermodynamic cycle analysis

Fuel and oxygen requirement

Coal-synthesized gas is used as fuel in the following power plant lay-out calculations. Table 1 shows the assumed molar composition of syngas gas (Winslow 1977). The lower heating value of syngas is 11.2 MJ/kg, which means that a continuous thermal power plant of 1,500 MW_{th} capacity requires a fuel flow rate of 133.93 kg/s. The mass flow rate of oxygen required to oxidize the syngas components, CO, H₂, and CH₄, is calculated from reactions (2)–(4), and the mass flow rate of NiO required to supply the required amount of oxygen is calculated from reaction (1). These calculations indicate that the oxygen consumption is 0.7402 kg per kg of fuel resulting in the formation of 0.5349 kg of H₂O and 1.2053 kg of CO₂ when fuel conversion is complete. The total stoichiometric oxygen requirement is 99.13 kg/s. In order to achieve complete fuel conversion, 8 % excess oxygen (Lyngfelt et al. 2001; Fan 2010) is provided resulting in a total oxygen flow rate of 107.06 kg/s through circulation of the active oxygen carrier.

Outline of the heat balance on the reactors

In the following cycle analysis, we assume that the oxygen carrier particles are perfectly mixed with gas stream, and the atmospheric CLC reactors are isothermal and that the conversion reactions reach 100 % completion (which is reasonably given that NiO-based oxygen carriers have achieved >99 % conversion for syngas (Li and Fan 2008)). Since the calculations of NiO flow rate are based on 8 % excess oxygen supply in the FR, 92.59 mass% of the NiO entering the FR is assumed to be converted to Ni. The heat or energy balance in the reactors is based on the idea that, in the absence of phase change, the sum of the sensible heat

Fig. 2 Arrangement of atmospheric chemical-looping combustion power plant

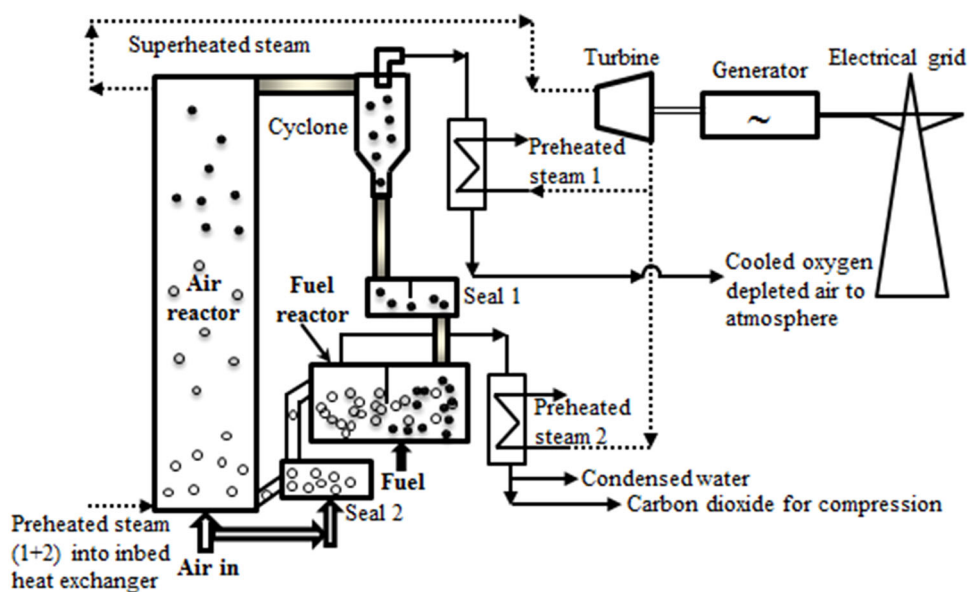


Table 1 Composition of coal synthesized gas

Species	Formula	Mole%
Hydrogen	H ₂	45.7
Carbon monoxide	CO	19.6
Methane	CH ₄	6.6
Carbon dioxide	CO ₂	28.1

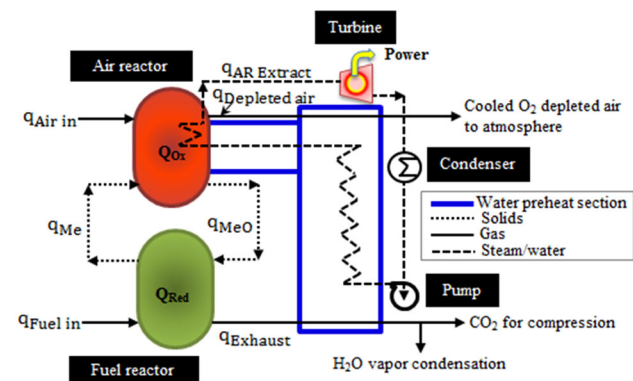


Fig. 3 Schematic diagram of atmospheric CLC energy balance model on the fuel side

of all the outgoing streams and the heat extracted, if any, by the embedded heat exchangers is equal to the sum of the sensible heat of the all the incoming streams and the heat of the reaction. A major portion of heat produced at AR by exothermic reaction is extracted using in-bed heat exchangers to superheat or reheat the steam coming from the preheaters. Based on the steady model shown in Fig. 3, the heat balance for the air and the FRs of the CLC system is expressed by Eqs. (5) and (6), respectively.

$$q_{Air\ in} + q_{Me} + q_{Ox} = q_{Depleted\ air} + q_{MeO} + q_{AR\ Extract} \quad (5)$$

$$q_{Fuel\ in} + q_{MeO} + q_{Red} = q_{Exhaust} + q_{Me} \quad (6)$$

In Eq. (5), terms q_{MeO} , q_{Me} , $q_{Air\ in}$, $q_{Depleted\ air}$ are, respectively, the thermal energy flow in oxygenated metal, reduced metal, air entering, and oxygen-depleted air leaving the AR. The terms q_{Ox} and q_{Red} are the heat of oxidation and reduction in the air and the FRs, respectively, and are calculated by multiplying mass of the reactive gas stream (O₂ or fuel) with the heat of reaction at reactor temperature. $q_{Fuel\ in}$ and $q_{Exhaust}$ are, respectively, the thermal energy flow in (of the fuel stream) and out (i.e., that of the carbon dioxide rich exhaust stream of FR). The term $q_{AR\ Extract}$ is the thermal energy extracted in the AR to generate high pressure and high temperature steam. The sign for term q_{Red} in Eq. (6) is positive for syngas and negative for natural gas. All energy terms are in MW. The sensible heat (fuel input of 1,500 MW_{th}) produced by a syngas (Q_{LHV}) as a result of the redox reactions is given by Eq. (7)

$$Q_{LHV} = q_{Ox} + q_{Red} \quad (7)$$

Thus, the thermal input (based on lower heating value) for syngas is calculated by subtracting q_{Red} term from q_{Ox} and, for natural gas, it is calculated by adding q_{Red} term to q_{Ox} .

Sensible heat of the stream i entering or leaving the CLC reactors is calculated from Eq. (8)

$$q_i = M_i \int_{T_r}^T C_{Pi}dT \quad (8)$$

Heat capacities (Nayef and Redhouane 2010) of the individual component in the gas stream are expressed in terms of the gas temperature, T , as

$$C_{p_i} = a + bT + cT^2 + dT^3 \quad (9)$$

Heat capacity of the active metal, Ni or NiO (Knacke et al. 1991) is calculated using Eq. (10)

$$C_{p_m} = \alpha + \beta T + \gamma T^{-2} \quad (10)$$

The heat capacity of the support material (NiAl_2O_4) is estimated by table (Barin 1989) of heat capacity values at wide range of temperatures by interpolation. Terms a , b , c , d as well as α , β , and γ are coefficients of temperature polynomial and are taken from the literature as cited above.

Results and discussion

Mass and energy balances on the furnace side

On the furnace side, five sub-systems have been considered, as shown schematically in Figs. 3 and 4. These are the AR (operating at 1 bar and 900 °C), the FR (operating at 1 bar and 908 °C), the air and the fuel preheaters, and the embedded heat exchangers in the AR through which heat is taken for steam generation. Mass flow rates of individual components through these sub-systems have been found by balancing moles of reactant and product using reactions (1)–(4) according to the mole fraction of fuel components. Energy (heat) balances have been made for a syngas-fueled CLC system of 1,500 MW_{th} fuel input using Eqs. (5)–(9). The resulting heat and mass flow rates into these sub-systems are shown in Fig. 4. Air at flow rate of 447.83 kg/s drawn to the CLC system and preheated air enters AR where 99.13 kg/s of oxygen in the air is selectively reacted with the reduced metal stream (consisting of 363.65-kg/s Ni, 37.02-kg/s NiO, and 333.20-kg/s NiAl_2O_4) to form metal oxide stream (consisting of 499.80-kg/s NiO and 333.20 kg/s of NiAl_2O_4). The major part of the heat, produced by highly exothermic reaction in the AR is removed (1,129.98 MW_{th}) by a heat exchanger embedded in the reactor. Heat produced (50.31 MW_{th}) by the mildly exothermic metal reduction reaction in the FR increases the FR temperature by 8 °C compared to the AR. 133.93 kg/s of the fuel (syngas) is preheated from 30 to 157 °C by 233.06 kg/s of the exhaust gas stream of the FR. A significant amount of sensible heat is still available in the depleted air stream from the AR and in the exhaust gases of the FR after preheating respective reactor inlet streams. These amount to 115.57 MW_{th} at 343 °C and 255.57 MW_{th} at 834 °C, respectively. These are used for feed water preheating as explained below.

Lay-out of the CLC power plant

The CLC power plant consists of two major sections: the atmospheric CLC reactors system and the supercritical

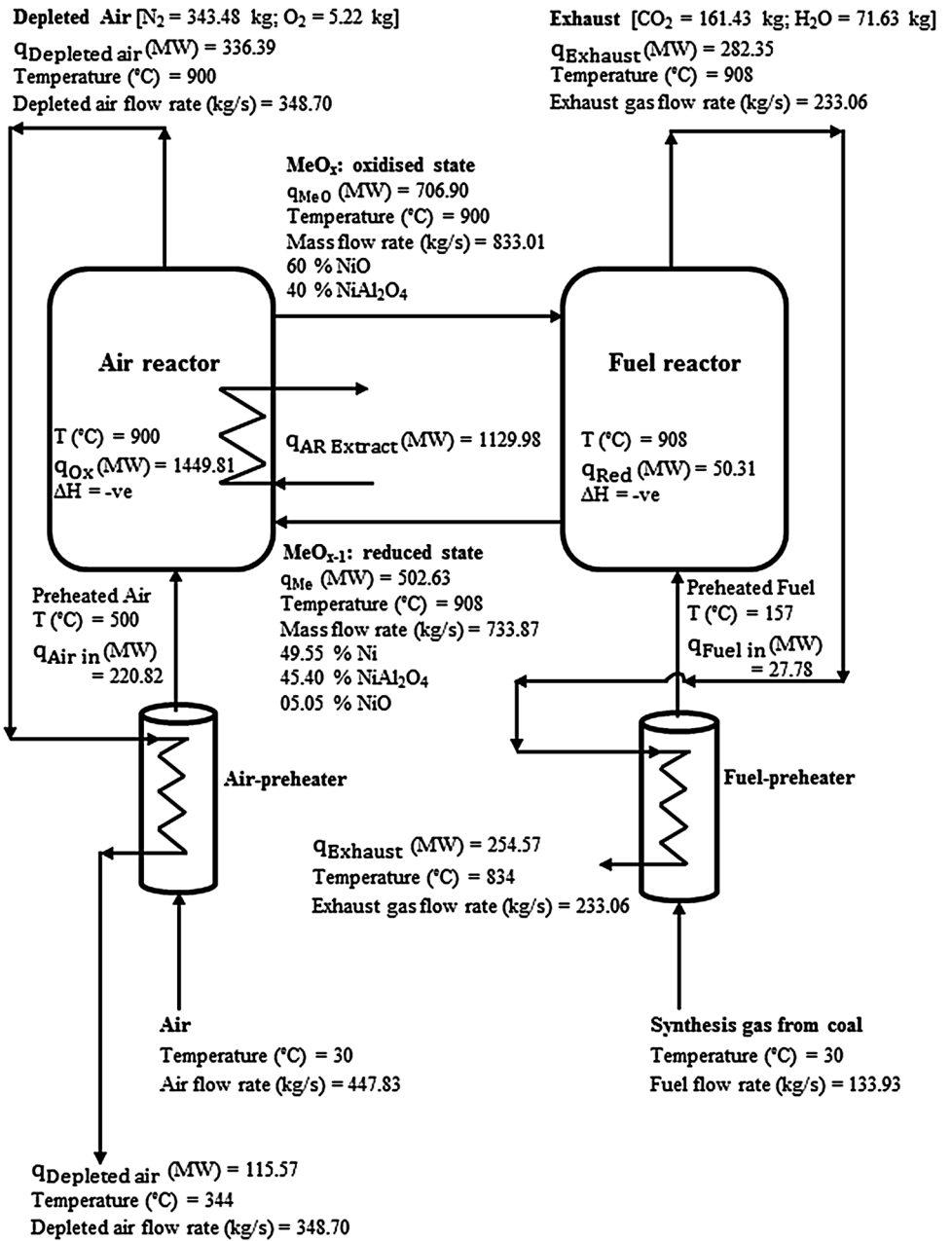
steam cycle system. The net heat generated during the redox reactions in the former is utilized by latter to produce high pressure and high temperature steam which drives a turbine and produces electrical energy. In the present analysis of the lay-out, the steam generation side is made to mimic the Rankine cycle-based supercritical steam cycle of a conventional boiler in terms of operating temperatures and pressures. A schematic of CLC power plant with the steam cycle arrangement is shown in Fig. 5. The proposed power plant configuration is unique in comparison with a conventional boiler in the sense that it uses the additional heat available from exhaust streams of the air and the FRs for feed water heating. A brief description of the various streams is given below.

Air from the atmosphere (a1) is drawn into the cycle and is fed to the air preheater where it gets heated by the oxygen-depleted air exhaust from the AR (a3) to a temperature of 500 °C. The preheated air (a2) then enters the AR where it picks up part of the heat from the exothermic reaction and gives up part of its oxygen content to come out as oxygen-depleted air (a3) at a temperature of 900 °C. It enters the air preheater and gives up part of its heat to come out at a temperature of 344 °C (a4). It then enters the first condensate (boiler feed water) heater where it gives up heat to come out at a temperature of 70 °C (a5).

The fuel (syngas) stream enters fuel preheater (f1) at a temperature of 30 °C and is preheated (f2) to a temperature of 157 °C before it enters the FR. There it gets oxidized by the metal oxide to form CO_2 and H_2O . The exhaust gas stream (e1) at a temperature of 908 °C enters the fuel preheater, and leaves it at a temperature (e2) of 834 °C. It then enters the second condensate (feed water) heater where it gives up its heat (e3) to exit at 101 °C after which it goes through a flue gas conditioner to extract steam. Condensed water (e5) is separated and pure CO_2 stream (e6) is compressed in four stage compressor unit to 110 bar (e7) and is sent for storage.

The steam generation system is similar to that of a conventional supercritical steam generator. A large portion of the heat produced by metal oxidation reaction inside the AR is taken away by embedded/in-bed heat exchangers to generate steam. These consist of HE1, which is the supercritical steam generator that also serves as the primary steam source, and HE2 and HE3 which serves as re-heaters and operate in the respective pressure and temperature range as explained below. The supercritical steam cycle is operated at 240 bar/538/552/566 °C (El-Wakil 2010). The supercritical steam (s6) from HE1 available at 240 bar and 538 °C enters the high pressure (HP) steam turbine and expands down to 55 bar at medium pressure (MP) steam turbine, and then to 14 bar at low pressure (LP) turbine. The optimum efficiency and steam quality at exit of LP turbine are key for choice of an appropriate reheat pressure (Naqvi

Fig. 4 Heat balance for syngas-fueled 1,500 MW_{th} CLC system



2006). More the reheat pressure, the lower is the steam quality at the LP turbine exit. The HP turbine exit stream (s7) is reheated from 305 to 552 °C (s8) using HE2, and the MP turbine exit steam (s9) is reheated from 332 to 566 °C (s10) by HE3. The condensate (0.069 bar at 39 °C) from LP turbine exit (s11) is divided into two streams (s12 and s13) as inlets to the pumps 1 and 2, respectively. The condensate pumps 1 and 2 pump the condensate to high pressure, and it flows through a series of feed water preheaters. High pressure (243.12 bar) water streams (s1 and s3) are preheated by depleted air (a4) and exhaust (e2) streams, respectively. Preheated streams (s2 and s4) are of same temperature and join to form a single stream (s5) at 240 bar

pressure. The T-s diagram showing the details of supercritical pressure steam cycle is given in Fig. 6. Cooled depleted air stream (a5) is left to atmosphere, while exhaust of the FR stream (e3) from fuel preheater is allowed to cool (e4) in flue gas conditioner to atmosphere temperature.

Provision for carbon capture and storage

The main advantage of a CLC-based power plant is that no additional energy is required to separate CO₂ from nitrogen as the flue gas is nitrogen-free. Nearly, a pure CO₂ stream is obtained by condensing the water vapor in the flue gas conditioner as shown in Fig. 5. In the proposed lay-out,

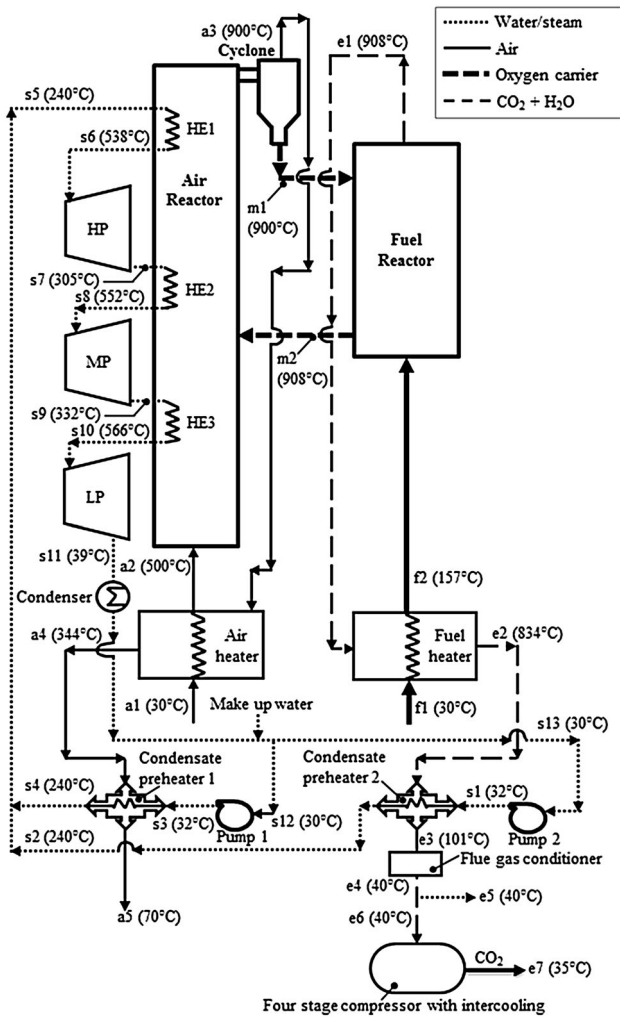


Fig. 5 Schematic diagram of syngas-fueled CLC steam cycle-based power plant lay-out

carbon will be captured (in the form of CO₂) once the fossil fuel (syngas) is converted into electrical energy prior to release in to the atmosphere. It is then compressed to 110 bar so that it can be transported over 100 km from the plant to a CO₂ disposal system, while still maintain its supercritical state (74 bar and 31.1 °C) so that the volume of the stored CO₂ is small. The possible storage (or sequestration) options include injecting supercritical CO₂ into deep geological formations at depths below about 800 m or injecting it into oil wells to enhance the oil recovery or even deep-sea disposal. The eventual disposal of CO₂ is not included in the present analysis; its capture and compression to 110 bar are, however, taken into in arriving at the mass and energy balances.

Overall energy balance

Detailed thermodynamic analysis for the overall power plant is presented in Table 2 for the syngas-fired CLC of

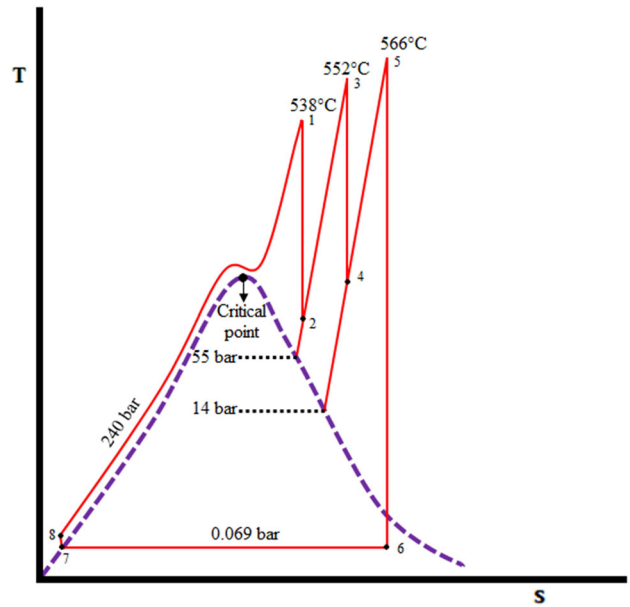


Fig. 6 Schematic T-s diagram of supercritical, double reheat 240 bar/538/552/566 °C ideal Rankine cycle for the CLCSC power plant

1,500 MW_{th} capacity. The mass flow rates, the temperature, pressure, and enthalpy of the streams at various points in the cycle are listed. From these values, which have been arrived at by assuming the thermodynamic processes to be ideal, the work done by various sub-systems, etc., can be calculated. A summary of the overall energy balance is given in Table 3. It can be seen that for an overall thermal input (in the form of the calorific value of the syngas) of 1,500 MW_{th}, the HP, the MP, and the LP turbines produce 129, 144, and 347 MW of electrical power. The power required for compression of CO₂ to 110 bar with intercooling is estimated to be 58 MW_e. The gross efficiency of syngas-fueled CLC power plant is calculated using Eq. (11)

$$\eta_{Gross} = \frac{P_{steam\ turbine}}{m_{fuel} \cdot LHV_{fuel}} \tag{11}$$

In Eq. (11), P_{steam turbine} is the total power produced by the three steam turbines in MW, m_{fuel} is mass flow of fuel in kg/s, and LHV_{fuel} is the lower heating value of fuel in MJ/kg. The calculated value of η_{Gross}, the gross efficiency of the CLCSC-based power plant is found to be 41.34 %. Recently, Reddy et al. (2014) evaluated the gross efficiency of a coal-fired supercritical steam cycle power plant to be 43.32 % for a condenser pressure of 0.07 bar, which is the same as that in the present study. The gross efficiency in the present study is lower because of the lower turbine inlet conditions of the steam, namely, pressure of 240 bar and temperature of 538 °C compared to those of 300 bar and 590 °C in the study of Reddy et al. (2014). The net efficiency (η_{Net}) in the present study is estimated from

Table 2 Detailed thermodynamic analysis of syngas-fueled 1,500 MW_{th} CLCSC-based power plant operating at 240 bar (538 °C) at HP, 55 bar (552 °C) at MP, and 14 bar (566 °C) at LP

Stream	P (bar)	T (°C)	m (kg/s)	h (kJ/kg)
Air				
a1	1.01	30	447.83	0.00
a2	1.01	500	447.83	493.08
a3	1.01	900	348.70	964.68
a4	1.01	344	348.70	331.39
a5	1.01	70	348.70	41.54
Fuel				
f1	1.01	30	133.93	0.00
f2	1.01	157	133.93	207.40
Exhaust				
e1	1.01	908	233.06	1211.47
e2	1.01	834	233.06	1092.29
e3	1.01	101	233.06	43.89
e4	1.01	40	233.06	18.74
e5	1.01	40	71.63	41.73
e6	1.01	40	161.43	8.54
e7	110	35	161.43	4.26
Water/steam				
s1	243.12	32	235.19	155.97
s2	243.12	240	235.19	1041.34
s3	243.12	32	97.06	155.97
s4	243.12	240	97.06	1041.34
s5	240	240	332.25	1041.06
s6	240	538	332.25	3312.27
s7	55	305	332.25	2922.83
s8	55	552	332.25	3550.66
s9	14	332	332.25	3117.56
s10	14	566	332.25	3619.79
s11	0.069	39	332.25	2573.72
s12	1.01	30	97.06	0.00
s13	1.01	30	235.19	0.00
O₂ carrier				
m1	1.01	900	833.01	848.61
m2	1.01	908	733.87	684.90

Eq. (12) which includes the power consumption cost for CO₂ compressors and for feedwater circulation.

$$\eta_{Net} = \frac{P_{steam\ turbine} - P_{CO_2\ comp} - P_{water\ pump}}{m_{fuel} \cdot LHV_{fuel}} \quad (12)$$

The net efficiency of power generation is, therefore, 36.77 % which includes the provision for CO₂ capture and compression to 110 bar. This value, which does not include thermodynamic irreversibilities, compares well with the net thermal efficiency of power generation using coal-fired sub-critical boilers.

Table 3 Overall energy analysis of 240 bar/538/552/566 °C CLCSC-based 1,500 MW_{th} power plant

Energy production/consumption	Power (MW _e)
High pressure turbine	129
Medium pressure turbine	144
Low pressure turbine	347
Total production	620
Power consumption for CO ₂ compression (110 bar)	58
Power consumption for water pumping	11
Total available power	552
Power plant efficiency	
Gross cycle efficiency	41.34
Net cycle efficiency	36.77

Conclusions

Using mass and energy balances, a lay-out of a syngas-fueled 1,500 MW_{th} CLC power plant has been made with detailed thermodynamic analysis. The lay-out is such that the steam side of the power plant is very similar to that of a conventional boiler in a thermal power plant. The lay-out of the furnace side is significantly different; the CLC mode of combustion necessitates the use of two reactors connected by a circulating oxygen carrier in the form of metal/metal oxide pellets. While the gas–solid reactions in both the reactors are exothermic, the lay-out has been made in such a way that only one of them, namely, the AR has in-bed heat exchangers, thus simulating the lay-out of a coal-fired CFB boiler. Provision has been made, through mass and energy balances, to allow for supercritical, superheated steam generation, and twice-reheated steam in the in-bed heat exchangers of the AR. The exhaust gases from the air and FRs are used to preheat the air and the fuel streams to these reactors as well as to preheat the condensate entering the boiler. With these arrangements, the net efficiency of the power plant is estimated to be 36.77 % which includes the provision for CO₂ capture and compression to 110 bar. This value, which does not include thermodynamic irreversibilities, compares well with the net thermal efficiency of power generation using coal-fired sub-critical boilers. Finally, the lay-out is such that it opens up the possibility of retrofitting a coal-fired CFB to operate in a CLC mode with provision for CCS; this, however, requires further study. In summary, it can be concluded that sustainable, clean, and efficient energy generation from coal appears to be feasible using chemical-looping combustion.

References

Adánez J, Abad A, Garcia-Labiano F, Gayan P, Diego DLF (2012) Progress in chemical-looping combustion and reforming technologies. Prog Energy Combust Sci 38:215–282

- Adánez J, de Diego LF, García-Labiano F, Gayán P, Abad A (2004) Selection of oxygen carriers for chemical-looping combustion. *Energy Fuel* 18:371–377
- Adánez J, García-Labiano F, de Diego LF, Gayán P, Abad A, Celaya J (2005) Development of oxygen carriers for chemical-looping combustion. In: Thomas DC, Benson SM(ed) Carbon dioxide capture for storage in deep geologic formations—results from the CO₂ capture project, Elsevier, Oxford (UK), Vol 1 Chapter 34 pp 587–604
- Adánez-Rubio I, Abad A, Gayán P, García-Labiano F, de Diego LF, Adánez J (2013) The fate of sulphur in the Cu-based chemical-looping with oxygen uncoupling (CLOU) process. *Appl Energy* 113:1855–1862
- Bandyopadhyay A (2011) Amine versus ammonia absorption of CO₂ as a measure of reducing GHG emission: a critical analysis. *Clean Technol Environ Policy* 13:269–294
- Barin I (1989) Thermochemical data of pure substances, part II. Hemisphere Publishing Corporation, New York
- Chikkatur, Ananth P, Ambuj D Sagar (2007) Cleaner power in India: towards a clean-coal-technology Road map. Discussion Paper 2006–2007, Mass.: Belfer Center for Science and International Affairs, Cambridge
- Damartzis T, Papadopoulos AI, Seferlis P (2014) Optimum synthesis of solvent-based post-combustion CO₂ capture flow sheets through a generalized modeling framework. *Clean Technol Environ Policy*. In press. doi:10.1007/s10098-014-0747-2
- Davison J, Thambimuthu K (2009) An overview of technologies and costs for carbon dioxide capture in power plants. *Proc IMechE Part A* 223:201–212
- El-Wakil MM (2010) Power plant technology. Tata McGraw Hill, New Delhi
- Fan LS (2010) Chemical-looping system for fossil energy conversions. Wiley, New Jersey
- Hasaneen R, Elasyed NA, Barrufet MA (2014) Analysis of the technical, microeconomic, and political impact of a carbon tax on carbon dioxide sequestration resulting from liquefied natural gas production. *Clean Technol Environ Policy*. In press. doi:10.1007/s10098-014-0735-6
- Hatanaka T, Matsuda S, Hatano H (1997) A new-concept gas-solid combustion system “MERIT” for high combustion efficiency and low emissions. In: Proceeding of the 32nd Intersociety energy conversion energy conference (IECEC-97). Honolulu, Hawaii; pp. 944–948
- IEA (2006) World energy outlook (2006) International Energy Agency (IEA). IEA Publishing Web. www.iea.org/publications/freepublications/publication/name,3650,en.html. Accessed 10 Dec 2014
- IEA (2013) Developments in circulating fluidised bed combustion, IEA Clean Coal Report No 13/7 June 2013. <http://www.iea-coal.org.uk/documents/83172/8753/Developments-in-circulating-fluidised-bed-combustion,-CCC/219>, Accessed 30 March 2014
- IPCC (2005) Special report on carbon dioxide capture and storage. Prepared by working group III of the intergovernmental panel on climate change. Cambridge University Press, New York
- Ishida M, Jin H (1994) A new advanced power-generation system using chemical-looping combustion. *Energy* 19:415–422
- Ishida M, Zheng D, Akehata T (1987) Evaluation of a chemical-looping combustion power-generation system by graphic energy analysis. *Energy* 2:147–154
- Jayanti S, Saravanan V, Sivaji S (2012) Assessment of retrofitting possibility of an Indian pulverized coal boiler for operation with Indian coals in oxy-coal combustion mode with CO₂ sequestration. *Proc IMechE Part A* 226:1003–1013
- Jenni KE, Baker ED, Nemet JF (2013) Expert elicitation of energy penalties for carbon capture technologies. *Int J Greenh Gas Control* 12:136–145
- Johansson M (2007) Screening of oxygen-carrier particles based on iron-, manganese-, copper and nickel oxides for use in chemical-looping technologies. Doctoral Thesis, Chalmers University of Technology, Göteborg, Sweden
- Kanniche M, Gros-Bonnivard R, Jaud P et al (2010) Pre-combustion, post-combustion and oxy-combustion in thermal power plant for CO₂ capture. *Appl Therm Eng* 30:53–62
- Knacke O, Kubaschewski O, Hesselmann K (1991) Thermochemical properties of inorganic substances. Springer, Berlin
- Krishna Priya GS, Bandyopadhyay S (2013) Emission constrained power system planning: a pinch analysis based study of Indian electricity sector. *Clean Technol Environ Policy* 15:771–782
- Kronberger B, Beal C, Morin JX, Hofbauer H (2004) Design, hydrodynamic testing and scale-up recommendations of a conceptual large-scale chemical-looping combustion power plant. In: Proceedings of the 3rd Conference on Carbon Sequestration. Alexandria, USA
- Li F, Fan LS (2008) Clean coal conversion processes—progress and challenges. *Energy Environ Sci* 1:248–267
- Linderholm C, Abad A, Lyngfelt A, Mattisson T (2008) 160 h of chemical-looping combustion in a 10 kW reactor system with a NiO-based oxygen carrier. *Int J Greenh Gas Control* 2:520–530
- Liszka M, Ziebig A (2010) Coal-fired oxy-fuel power unit process and system analysis. *Energy* 35:943–951
- Loughlin DH, Yelverton WH, Dodder RL, Miller CA (2013) Methodology for examining potential technology breakthroughs for mitigating CO₂ and application to centralized solar photovoltaics. *Clean Technol Environ Policy* 15:9–20
- Lyngfelt A, Leckner B, Mattisson T (2001) A fluidized bed combustion with inherent CO₂ separation; application of chemical-looping combustion. *Chem Eng Sci* 56:3101–3113
- Lyngfelt A, Kronberger B, Adánez J, Morin JX, Hurst P (2004) Development of oxygen carrier particles for chemical-looping combustion, design and operation of a 10 kW chemical-looping combustor. In: Proceeding 7th Int conference of greenhouse gas control technology (GHGT-7). Vancouver, Canada
- Markström P, Linderholm C, Lyngfelt A (2013) Operation of a 100 kW chemical-looping combustor with Mexican petroleum coke and Cerejon coal. *Appl Energy* 113:1830–1835
- Mayer F, Bidwe AR, Schopf A, Taheri K, Zieba M, Scheffknecht G (2013) Comparison of a new micaceous iron oxide and ilmenite as oxygen carrier for chemical-looping combustion with respect to syngas conversion. *Appl Energy* 113:1863–1868
- Moldenhauer P, Rydén M, Mattisson T, Younes M, Lyngfelt A (2013) The use of ilmenite as oxygen carrier with kerosene in a 300 W CLC laboratory reactor with continuous circulation. *Appl Energy* 113:1846–1854
- Naqvi R (2006). Analysis of natural gas-fired power cycles with chemical-looping combustion for CO₂ capture. Doctoral Thesis, NTNU, Trondheim, Norway
- Nayef G, Redhouane H (2010) Principles of chemical engineering processes. CRC press, New York
- Reddy VS, Kaushik SC, Tyagi SK (2014) Energetic analysis and evaluation of coal-fired supercritical thermal power plant and natural gas-fired combined cycle power plant. *Clean Technol Environ Policy* 16:489–499
- Seepana S, Jayanti S (2009) Optimized enriched CO₂ recycle oxy-fuel combustion for high ash coals. *Fuel* 102:32–40
- Sivaji S, Jayanti S (2010) Steam-moderated oxy-fuel combustion (SMOC). *Energy Convers Manag* 51:1981–1988
- Ströhle J, Orth M, Epple B (2013) Design and operation of a 1 MW_{th} chemical-looping plant. *Appl Energy* 113:1490–1495
- Tong A, Bayham S, Kathe VM, Zeng L, Luo S, Fan LS (2013) Iron-based syngas chemical-looping process and coal-direct chemical looping process development at Ohio State University. *Appl Energy* 113:1836–1845

- VTT (2013) Utility scale CFB for competitive coal power: CFB800. www.vtt.fi/files/sites/flexiburncfb/cfb800_brochure.pdf, Accessed 30 March 2014
- Wall TF (2007) Combustion processes for carbon capture. *Proc Combust Inst* 31:31–47
- Wall T, Liu Y, Spero C et al (2009) An overview on oxyfuel coal combustion—state of the art research and technology development. *Chem Eng Res Des* 87:1003–1016
- Winslow AM (1977) Numerical model of coal gasification in a packed bed, Symposium (international) on combustion, Vol 16 pp. 503–513
- Yan J, Chou SK, Desideri U, Tu ST, Jin HG (2013) Research, development and innovations for sustainable future energy systems. *Appl Energy* 112:393–395